Proton Diffusion Mechanism in Amorphous SiO_2

Julien Godet and Alfredo Pasquarello

École Polytechnique Fédérale de Lausanne (EPFL), Institute of Theoretical Physics, CH-1015 Lausanne, Switzerland
Institut Romand de Recherche Numérique en Physique des Matériaux (IRRMA), CH-1015 Lausanne, Switzerland

(Received 21 June 2006; published 13 October 2006)

We study proton diffusion in amorphous SiO_2 from the atomic scale to the long-range percolative regime. *Ab initio* molecular dynamics suggest that the dominant atomic process consists in cross-ring interoxygen hopping assisted by network vibrations. A statistical analysis accounting for the disorder in amorphous SiO_2 yields relations between transition energies and interoxygen distances for both cross-ring and nearest-neighbor hopping. The percolative regime is then addressed through large-size model systems reproducing these relations. Cross-ring hopping is confirmed as the dominant diffusion mechanism and supported by a good agreement with experiment for the activation energy.

DOI: 10.1103/PhysRevLett.97.155901 PACS numbers: 66.30.Jt, 61.43.Er, 71.15.Pd

The mobility of impurities in disordered oxides is a theme of fundamental interest but also carries great practical relevance for metal-oxide-semiconductor devices. In particular, one of the most studied impurities is the ubiquitous hydrogen species. In electronic devices, its occurrence critically reduces the interface defect density to meet operational requirements [1,2]. However, hydrogen is also suspected to cause performance degrading, such as due to interface charging [3–6] or to the onset of dielectric breakdown [7–9]. A common process at the origin of these phenomena is the migration of hydrogen, most likely in the mobile form of protons. However, fairly little is known to date about the atomistic mechanism of this process. The understanding is complicated by the strong interaction between the proton and its host network, whereby the disordered nature of the oxide structure cannot be ignored.

McLean proposed a migration model in which the proton hops between first-neighbor oxygen atoms in amorphous SiO_2 (Fig. 1) [10]. Through a comparison with experimental data on the charging of interface traps, he then derived an activation energy of about 0.85 eV. This result was subsequently supported by both experimental [11–14] and theoretical studies [3,15]. However, Devine and Herrera recently addressed the proton mobility by directly sensing charge displacements [16]. Despite the limited range of studied temperatures, their data clearly indicated a significantly lower activation energy and hopping lengths well beyond first-neighbor oxygen distances. These results led to the suggestion of an alternative diffusion mechanism based on cross-ring hopping (Fig. 1). However, it is not clear how these ideas reconcile with previous theoretical work [3,15].

In this Letter, we provide a picture of proton diffusion in amorphous SiO_2 (a-SiO_2) covering the process from the atomic scale to the long-range percolative regime. First, to get insight into the relevant atomistic processes, we perform *ab initio* molecular dynamics in a realistic disordered oxide model. Our simulation suggests cross-ring hopping assisted by network vibrations. Through static calculations, we then carry out a statistical analysis of the hopping energetics in our model and identify a relation between energy barriers and hopping lengths, for both cross-ring and first-neighbor hopping. The percolative regime is addressed via large-size model systems reproducing these energetic relations. This application confirms the predominance of cross-ring hopping and yields an estimate of the activation energy for the percolative regime in accord with Devine and Herrera [16].

We described the electronic structure within a generalized gradient approximation to density-functional theory [17]. We used a norm-conserving pseudopotential for Si [18] in conjunction with ultrasoft pseudopotentials for H and O [19]. The electron wave functions and charge density were described by plane wave basis sets with cutoffs of 24 and 150 Ry, respectively [20]. The Brillouin zone was sampled at the Γ point. Structural relaxations were achieved through damped molecular dynamics [21]. In this work, the quantum motion of the proton is neglected. Consideration of this effect is expected to lower the transition barriers by only $\sim$0.1 eV [15]. Moreover, a recent study of proton diffusion in water demonstrates that quantum effects do not affect the physical picture underlying the hopping mechanism [22].

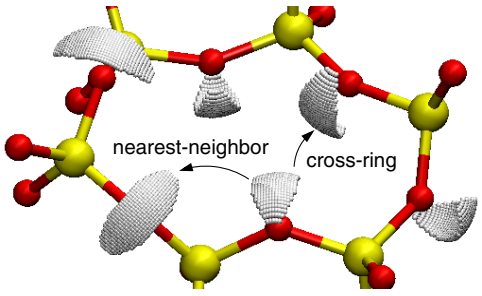

FIG. 1 (color online). Competitive proton hopping mechanisms in amorphous SiO_2. The caps around the O atoms schematically delimit the regions accessible to protons excited by at most 0.4 eV from their local equilibrium position.

For investigating the energetics in a-SiO_2, we used a disordered 72-atom model structure obtained previously [23]. The proton usually binds to bridging O atoms which become threefold coordinated with O-H^+ bond lengths of $\sim$1.0 Å (Fig. 1) [24]. For a Fermi level at the top of the valence band, the proton formation energy is 3.6 eV lower than the neutral H atom (with a spread of 0.23 eV). These results do not differ significantly from similar studies on crystalline SiO_2 [24]. More rarely, the disorder in our model allows for another kind of equilibrium configuration, in which an O-H^+-O complex forms between two bridging O atoms across a ring. The formation of such a complex stabilizes the proton by $\sim$0.3 eV.

We evaluated the strength of the O-H^+ bonding by placing the detached proton at the center of the largest interstitial void in our model (radius of 3.5 Å). This gave a detachment energy of 4.9 eV, indicative of a strong bond. We then further characterized the properties of the O-H^+ bonding by describing the energetics of the proton around the bridging O atom. We evaluated energy variations for varying orientations of the O-H^+ bond while keeping the O-H^+ distance fixed at 1.0 Å. We observed that the energy rapidly increases when the proton tilts toward one of the two neighboring Si atoms: typically, an increase by 0.4 eV is achieved for an angular displacement of 25° (Fig. 1). At variance, the evolution of the proton within the midplane of these Si atoms involves a much lower energy cost, an increase by 0.4 eV corresponding now to an angular displacement of 68° (Fig. 1). This flexibility originates from the fact that the threefold coordinated O atom preserves the angles between its ligands. The directionality of the proton motion hinders the hopping between nearest-neighbor O atoms (Fig. 1), despite their relatively short distance (2.6 Å).

To get insight into the dynamical properties of the proton in a-SiO_2, we performed *ab initio* molecular dynamics [21,25]. As initial positions for the proton, we considered three different O atoms, in order to explore the largest possible region in the simulation cell. In each case, we followed the atomic motion for a period ranging between 10 and 15 ps. We fixed the temperature at 1500 K, slightly higher than in typical oxidation conditions (1000–1400 K), but lower than the experimental melting point (2000 K). This is a reasonable compromise to observe interesting evolutions on the time scale of our simulations.

The usual condition for the proton in the simulation corresponds to a motion around its equilibrium position. Figure 2 shows a narrow distribution for the O-H^+ bond length (with a mean of 1.1 Å and a spread of 0.1 Å). The trajectories are predominantly confined within the Si-Si midplane (Fig. 2), as expected on the basis of our static calculations. We also show in Fig. 2 the distribution of O-H^+ distances taken with respect to the equilibrium position of the O atom. This distribution is significantly larger than that for the O-H^+ bond length, reaching distances up to 2.2 Å. These results indicate that lattice vibrations contribute significantly to the absolute displacement of protons and should be accounted for in the atomistic description of the hopping mechanism.

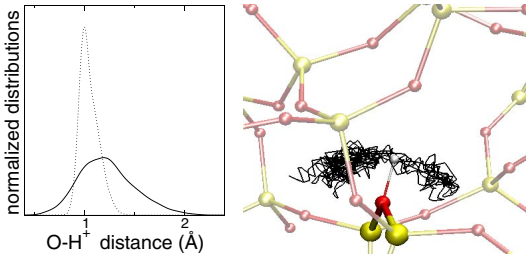

FIG. 2 (color online). Proton displacements in the molecular dynamics. Left: O-H^+ bond length distribution (dotted line), proton displacement with respect to the fixed equilibrium position of the O atom (solid line). Right: proton trajectory; the balls indicate the equilibrium sites.

All simulations showed qualitatively similar evolutions in which cross-ring hops brought the proton to visit 5 to 8 different O atoms, depending on its initial position. Hops between nearest-neighbor O atoms were not observed. To exemplify a typical hopping event, we give in Fig. 3 the evolution of the involved O-H^+ distances vs time. Before the hop, the proton is linked to the oxygen atom O_I, with a bond length of $\sim$1 Å, while the oxygen atom O_{II} is relatively far away. Then, the distance between the proton and O_{II} decreases and becomes about equal to that between the proton and O_I. After a period of 0.1 ps in which the proton is shared by the two O atoms, the hop is completed and the proton is found to be attached only to O_{II}.

We remark that the proton hop in Fig. 3 occurs only when the O_I-O_{II} distance is about 2.3 Å. By analyzing the proton trajectories in our simulations, we observed that

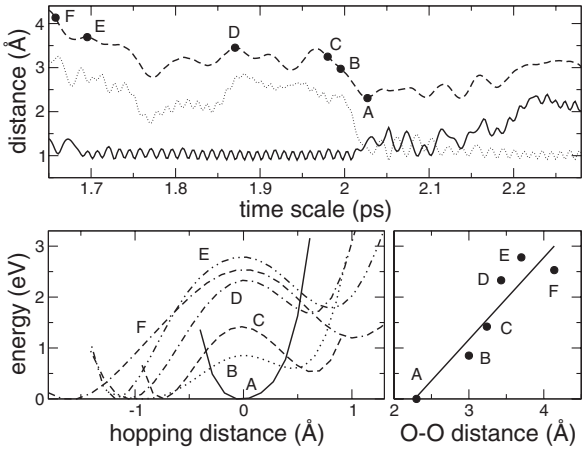

FIG. 3. Proton hopping between the oxygen atoms O_I and O_{II}. Upper panel: evolution of the O_I-H^+ (solid line), O_{II}-H^+ (dotted line), and O_I-O_{II} (dashed line) distances vs time. Lower left panel: energy barrier to move the proton from O_I to O_{II} for frozen instantaneous atomic configurations taken from the molecular dynamics (labeled by A–F cf. upper panel). Lower right panel: hopping barrier vs O_I-O_{II} distance.

hops always occurred in correspondence of such O-O distances (2.3 ± 0.1 Å). Thus, the hopping mechanism involves a transient complex in which the proton is shared by two O atoms, as found for certain equilibrium configurations. The formation of the intermediate O-H^+-O complex, in which the proton forms two bonds, favors the ensuing breaking of the strong O-H^+ bond. A similar mechanism for breaking strong bonds has also been observed for proton diffusion in water [26] and for network oxygen diffusion at the Si-SiO_2 interface [27].

To understand the hopping energetics, we select from our simulation a sequence of instantaneous atomic configurations (A–F) in which the distance between O_I and O_{II} progressively varies from 4.1 Å to the hopping distance of 2.3 Å (Fig. 3). For each configuration, we evaluated the energy profile for the proton moving between O_I and O_{II} in a frozen atomic structure. We found a typical double well potential in which the transition barrier decreases and finally vanishes as the O atoms approach (Fig. 3). The barriers are found to increase rapidly with the O_I-O_{II} distance [28], a direct consequence of the O-H^+ bond strength. Thermal energy considerations indicate that protons at room temperature can only hop if the O separation remains very close to 2.3 Å. In a-SiO_2, typical cross-ring O-O distances range between 2.5 and 4.0 Å, thereby implying that the only thermal energy of the proton is not sufficient to allow for long-range diffusion.

Transition energies for cross-ring proton hopping were therefore evaluated allowing for full structural relaxations. To permit a statistical analysis, we adopted a simplified procedure for the search of transition energies. For a given pair of O atoms, we identified the transition structure by constraining the interoxygen distance in the O-H^+-O complex to 2.3 Å while relaxing all other structural parameters. In a few cases, we also evaluated the barrier through a dragging procedure finding differences of at most 0.1 eV. The calculated transition energies show a linear trend when plotted against the O-O separation (Fig. 4). The relative orientation of the involved Si-O-Si bridges or the flexibility of the network in the vicinity of the transition path also affects the chemistry of O-H^+-O complex and is responsible for the spread with respect to the linear interpolation in Fig. 4. On average, transition energies in Fig. 4 are reduced by a factor of ~ 3 with respect to the trend in Fig. 3 for corresponding O-O distances, highlighting the role of network vibrations in activating proton diffusion.

On the time scale of our molecular dynamics simulations, we did not observe hopping between nearest-neighbor O atoms, in agreement with our static analysis (Fig. 1). However, for completeness, we also evaluated energy barriers for proton hopping between nearest-neighbor O atoms. For several O pairs, we defined a reaction coordinate for the proton motion and obtained the energy barrier allowing for full relaxation. As shown in Fig. 4, the transition energies calculated for nearest-neighbor hopping are also found to increase with O-O distance [29]. Transition barriers for nearest-neighbor hopping are generally larger than for cross-ring hopping. However, nearest-neighbor hopping at small O-O distances appears competitive with large-jump, cross-ring hopping.

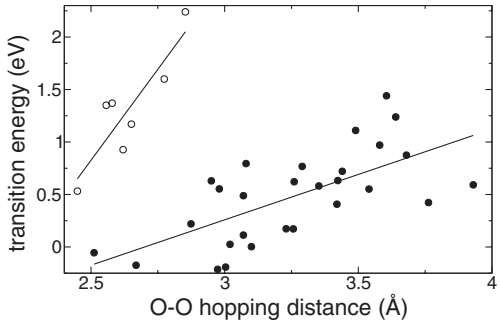

FIG. 4. Energy barrier vs O-O distance for cross-ring (full symbols) and nearest-neighbor hopping (open symbols) in a-SiO_2. The O-O distance corresponds to the relaxed a-SiO_2 structure (prior to proton insertion). Transition energies are referred to the average equilibrium energy of the proton. The lines correspond to linear regressions. We found spreads of 0.32 and 0.26 eV for cross-ring and nearest-neighbor hopping, respectively.

For the long-range diffusion, it is necessary to address length scales that are beyond the scope of density-functional calculations. We adopt a large-size structure of a-SiO_2 generated by classical molecular dynamics [30], which provides a good representation of interoxygen distances. This structure contains 1002 atoms in a periodic cubic cell of side of 24.5 Å. Proton transitions between all pairs of O atoms lying within 4.3 Å are admitted. To reproduce the energetic trends found in our density-functional analysis, we first assigned transition energies depending on the interoxygen distance following the linear regressions in Fig. 4. Each energy barrier is then randomly modified according to a Gaussian distribution reproducing the spread found in our density-functional calculations (Fig. 4). Nearest-neighbor and cross-ring connections are distinguished and treated with their respective linear regressions and spreads. In this way, we generated a large statistical ensemble of model systems with stochastically determined energy barriers.

The long-range diffusion can be pictured as a percolative motion. As shown by Roling for cubic lattices with random barriers [31], an estimate of the activation energy can be obtained by determining the energy for which the percolation cluster becomes infinite. For a given energy E, the size of the percolation cluster is determined by considering the largest distance between equilibrium sites that can be connected overcoming energy barriers lower than E. In Fig. 5, we show the evolution of the size of the largest percolation cluster vs the transition energy E. For diffusive motions ranging over distances of the order of the size of the model structure, we inferred an activation energy of 0.50 ± 0.03 eV, in good agreement with the experimental

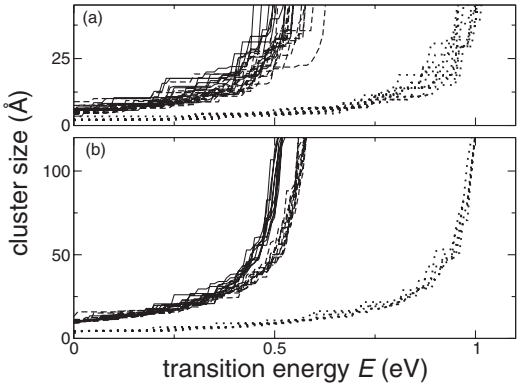

FIG. 5. Size of percolation cluster vs transition energy E admitting only cross-ring (dashed line) or only nearest-neighbor hopping (dotted line), or both combined (solid line), for a statistical set of model systems with (a) 10^3 and (b) 10^6 atoms.

value of 0.38 eV determined recently by sensing charge displacements [16].

We also addressed the issue of the dominant transition mechanism. The respective role of cross-ring and nearest-neighbor hopping was investigated by selectively closing one of the channels (Fig. 5). In the absence of nearest-neighbor hopping, the activation energy changed only slightly (0.55 ± 0.03 eV). On the other hand, the activation energy increased considerably (0.99 ± 0.02 eV) when the cross-ring mechanism was deactivated. This analysis clearly supports the dominant role of the cross-ring hopping mechanism for proton diffusion in a-SiO_2.

To address finite-size effects, we considered a set of models obtained by repeating 10 times the original atomic structure in every Cartesian direction. This yields model systems of a million atoms in a cubic cell of 245 Å. All energy barriers are reassigned following the same procedure applied to the smaller model [32]. As can be seen in Fig. 5, the divergences for these large models fall within at most 0.02 eV from those for the smaller models. This confirms the picture of the diffusion mechanism that we inferred.

In conclusion, our study reveals the mechanism governing the long-range proton diffusion in a-SiO_2 through a multiscale analysis which takes its origin at the atomic scale. Our work highlights the importance of properly accounting for structural disorder when interpreting diffusion processes in amorphous systems.

We thank A. Bongiorno and P. Broqvist for fruitful interactions, and K. Vollmayr and W. Kob for providing SiO_2 models [30]. Support from the SNF (Grant No. 200021-103562) is acknowledged. Calculations were performed at EPFL (DIT and CSEA) and CSCS.

[1] S. C. Witczak, J. S. Suehle, and M. Gaitan, Solid-State Electron. **35**, 345 (1992).
[2] A. Stesmans and V. V. Afanas'ev, J. Phys. Condens. Matter **10**, L19 (1998).
[3] S. T. Pantelides *et al.*, IEEE Trans. Nucl. Sci. **47**, 2262 (2000).
[4] K. Vanheusden and R. A. B. Devine, Appl. Phys. Lett. **76**, 3109 (2000).
[5] V. V. Afanas'ev, G. J. Adriaenssens, and A. Stesmans, Microelectron. Eng. **59**, 85 (2001).
[6] V. V. Afanas'ev, F. Ciobanu, G. Pensl, and A. Stesmans, Solid-State Electron. **46**, 1815 (2002).
[7] P. E. Blöchl and J. H. Stathis, Phys. Rev. Lett. **83**, 372 (1999).
[8] V. V. Afanas'ev and A. Stesmans, J. Electrochem. Soc. **146**, 3409 (1999).
[9] M. Houssa, A. Stesmans, R. J. Carter, and M. M. Heyns, Appl. Phys. Lett. **78**, 3289 (2001).
[10] F. B. McLean, IEEE Trans. Nucl. Sci. **27**, 1651 (1980).
[11] R. E. Stahlbush, R. K. Lawrence, and H. L. Hughes, IEEE Trans. Nucl. Sci. **45**, 2398 (1998).
[12] D. B. Brown and N. S. Saks, J. Appl. Phys. **70**, 3734 (1991).
[13] N. Saks, C. Dozier, and D. Brown, IEEE Trans. Nucl. Sci. **35**, 1168 (1988).
[14] K. Vanheusden *et al.*, Nature (London) **386**, 587 (1997).
[15] H. A. Kurtz and S. P. Karna, IEEE Trans. Nucl. Sci. **46**, 1574 (1999).
[16] R. A. B. Devine and G. V. Herrera, Phys. Rev. B **63**, 233406 (2001).
[17] J. P. Perdew *et al.*, Phys. Rev. B **46**, 6671 (1992).
[18] G. B. Bachelet, D. R. Hamann, and M. Schlüter, Phys. Rev. B **26**, 4199 (1982).
[19] D. Vanderbilt, Phys. Rev. B **41**, 7892 (1990).
[20] A. Pasquarello *et al.*, Phys. Rev. Lett. **69**, 1982 (1992); K. Laasonen *et al.*, Phys. Rev. B **47**, 10 142 (1993); we used the implementation in the QUANTUM-ESPRESSO package.
[21] R. Car and M. Parrinello, Phys. Rev. Lett. **55**, 2471 (1985).
[22] D. Marx, M. E. Tuckerman, and M. Parrinello, J. Phys. Condens. Matter **12**, A153 (2000).
[23] J. Sarnthein, A. Pasquarello, and R. Car, Phys. Rev. B **52**, 12 690 (1995); Phys. Rev. Lett. **74**, 4682 (1995).
[24] J. Godet and A. Pasquarello, Microelectron. Eng. **80**, 288 (2005).
[25] We used a fictitious mass of 250 a.u. and a time step of 10 a.u.
[26] M. E. Tuckerman, D. Marx, and M. Parrinello, Science **275**, 817 (1997).
[27] A. Pasquarello, M. S. Hybertsen, and R. Car, Nature (London) **396**, 58 (1998).
[28] Our results agree with cross-ring hopping in α-quartz [P. E. Bunson *et al.*, IEEE Trans. Nucl. Sci. **46**, 1568 (1999)].
[29] For typical intertetrahedral O-O distances, our results agree with previous calculations [3,15,28].
[30] K. Vollmayr, W. Kob, and K. Binder, Phys. Rev. B **54**, 15 808 (1996).
[31] B. Roling, Phys. Rev. B **61**, 5993 (2000).
[32] Since the stochastic spread is of the same order as transition-energy variations (Fig. 4), our assignment of barriers effectively breaks the structural periodicity.